Spring 5-3-2011

Hydrodynamics of a Cluster Descending at the Wall of a CFB Riser - Numerical Study

John R. Grace
University of British Columbia, jgrace@chml.ubc.ca

Subhashini Vashisth
University of British Columbia

HYDRODYNAMICS OF A CLUSTER DESCENDING AT THE WALL OF A CFB RISER: NUMERICAL STUDY

Subhashini Vashisth and John R. Grace
Department of Chemical and Biological Engineering,
University of British Columbia, 2360 East Mall, Vancouver, Canada V6T 1Z3

ABSTRACT
The incompressible hydrodynamics of a single parabolic cluster descending at the wall of a CFB riser was numerically simulated using a 2-D Eulerian-Granular model and a segregated time-dependent unsteady solver. Numerical predictions of the velocity of descent and the evolution of cluster shape are in reasonable agreement with experimental results available in the literature.

INTRODUCTION

Clustering of particles is an important feature observed in CFB risers. Grace and Tuot (1) showed that vertical flow of homogeneous particle suspensions is unstable, causing the particles to gather in 'clusters', 'strands' or 'packets', mostly falling down along the riser wall (2,3). The frequent formation, descent and dissolution of clusters causes axial dispersion of particles and gas, thereby having a negative impact on the performance of CFB catalytic and gas-solid reactions. Clustering also strongly influences particle holdup and pressure drop (4). In order to understand cluster dynamics, several researchers (e.g. 5, 6) have measured the velocity of descent of particle clusters near the wall of CFB risers. Except for very large risers, the descent velocities have almost always been found to be between 0.3 to 2.0 m/s, despite wide variations in operating conditions. Experimental investigations have also been reported on flow characterization of clusters (7, 8, 9), cluster porosity, cluster occurrence frequency, as well as cluster residence time and size (10, 11, 12). Despite significant advances in the visualization of flow, there is no clear definition of cluster shape. Yerushalmi (13) adopted the terms "streamers", "strands" and "ribbons". Rhodes et al. (14) described clusters as \`swarms or \`strands, depending on their shape and the operating conditions. Elliptical or ellipsoidal frontal shapes were observed by Lim et al. (6). Similarly, rounded-bottom assemblies descending near the riser wall were captured by the infrared images of Noymer and Glicksman (11). Even though the clusters are far from spherical in shape, some researchers (e.g. 15) have approximated clusters as spheres in order to simplify the analysis of gas flow around clusters.

Considering possible shapes of clusters, it seems reasonable from the existing information to assume aerodynamic bluff bodies. In the present work we have attempted to investigate a single cluster which, based on the experimental observations of Zhou et al. (5), is initially parabolic in shape. The leading edge of the descending cluster is assumed to be similar to that of a large liquid drop (6). A two-dimensional computational fluid dynamic model employing the Eulerian-granular model is used to simulate the behaviour of clusters. Numerical simulations based on the commercial CFD code solver, Ansys-Fluent 12.1, were carried out and are compared with the experimental results of Zhou et al. (5) and Lim et al. (6).

EULERIAN-GRANULAR GAS-SOLID FLOW MODEL

The gas-solid two-phase incompressible flow is modeled in an Eulerian-Granular framework, with the Syamlal-O'Brien (16) drag model employed for interphase momentum exchange. The solid phase stress was computed from the kinetic theory of granular flow. A laminar viscous model was assumed. External forces, lift and virtual mass forces were neglected. For the sake of brevity, the model equations are not presented here. Instead, the complete set of governing equations may be obtained from the manuals of Ansys-Fluent 12.1 (17). Table 1 specifies the granular parameters for the riser flow simulations. The value of the granular temperature was adopted from the literature (17, 18). Its value was kept constant as the core region of the riser was very dilute compared to the cluster. Hence, random fluctuations were neglected. Incorporation of an appropriate turbulence model and effect of varying the granular temperature will be considered in future work.

MODEL SET-UP AND NUMERICAL SOLUTION PROCEDURE

The CFB riser geometry and grid were created using Ansys-Workbench 12.1. The primary objective of the present work was to simulate the descent of an initially parabolic-shaped cluster of width D_c in a two-dimensional calculation region. Key parameters are listed in Table 2. Air and particles are fed into the riser from the bottom at a specified superficial gas velocity and at a given mass flux, respectively. Both particles and air leave the riser at the top. Initially, the riser was completely filled with air, and then the solids were introduced. At t = 0 s, the cluster was initiated. QUICK and second-order upwind differences were used to discretize the continuity and momentum equations respectively, whereas time was second-order implicitly discretized. The Phase-Coupled SIMPLE algorithm was used for pressure-velocity coupling. Each case was simulated for 1.5 s. The velocity of descent of each cluster was calculated as a mass-weighted-average velocity over all of the particles which initially belonged to the cluster, i.e.

$$U_{cl} = \left(\sum_{i=1}^{n} \varepsilon_{pi} \rho_p U_{pi} \right) / \left(\sum_{i=1}^{n} \varepsilon_{pi} \rho_p \right)$$

Boundary Conditions:

Uniform-velocity inlet conditions were imposed:

$U_{g,y} = U_g$; $U_{g,x} = 0$; $U_{p,y} = U_p$; $U_{p,x} = 0$

At the outlet: $\partial U_{g,y} / \partial y = \partial U_{g,x} / \partial y = 0$

No slip was imposed on the gas velocity at both side walls: $U_g = 0$

Transient simulations with a time step of 0.0001 s were carried out based on the governing equations and boundary conditions until steady state was obtained. In order to accurately account for the motion of clusters at the wall, refined grid spacing was used near the wall. Sensitivity to the grid spacing and time step were checked in the initial numerical experiments. The numerical computations were confirmed to be converged by checking the time-averaged mass residual ($<10^{-4}$) at different planes along the height of the riser. Simulation experiments were performed for 25 x 80 (width x height), 36 x 100 and 60 x 200 mesh resolutions and compared with the experimental results of Zhou et al. (5). This comparison showed that the 36 x 100 grid (with a time step of 0.0001 s) was able to provide mesh-independent results, as shown in Figure 1. This mesh was then adopted for further parametric studies.

RESULTS AND DISCUSSION

Experimental investigations of particle velocity profiles and motion of clusters near the wall of a 146 mm x 146 mm square by 9.14 m tall riser conducted by Zhou et al. (5) and Lim et al. (6) were compared with the CFD predictions. As can be seen from Figure 1, the air and particle velocity distributions were predicted reasonably well.

The particles inside the riser are not uniformly distributed, despite the imposed uniformity at the inlet. The clusters are characterised by local high particle concentration. The predicted spatial-temporal structure of clusters depends on the local velocities and concentrations of both gas and solids. Figure 2 shows predicted contours of particle volume fraction at various times for U_g = 5.5 m/s and G_s = 20 kg/m^2.s. A section of the riser is shown with a cluster at the wall. At t = 0.05 s, the volume fraction at the core of the cluster is 0.335, decreasing to 0.035 on its outer surface, and further to 0.029 at the centre of the riser. The cluster is predicted to descend along the wall of the riser and to deform under the influence of gravity and drag due to the upward flow of gas and solids. After t = 0.4 s, the outer surface of the cluster is pulled upwards, while the core maintains a drop-like elongated shape. The cluster is predicted to become more and more dilute with time as it expands, but it still keeps itself intact as a cluster, in practice probably influenced by inter-particle forces (20). The influence of frictional forces was neglected in this study. At t = 0.7 s, a petal-like shape was observed, after which the cluster starts to recede to a parabolic-drop shape, before detaching from the wall at $t \approx 0.8$ s. Similar shape evolution was predicted for other gas velocities and solid mass fractions.

The descent velocities of clusters for different gas velocities and solid mass fluxes are plotted in Figure 3 as a function of time. These velocities are predicted to be in the range of 0.1 to 2 m/s, in accordance with experimental values (e.g. 5, 6). The cluster velocity increases with time as the cluster descends from rest, before detaching from the wall. Increasing either the superficial air velocity or the solid mass flux in the upward direction increases the drag resistance on the descending cluster, thereby reducing its velocity of descent. Moreover, clusters are predicted to detach earlier with increasing upward suspension velocities and solids fluxes.

The predicted particle concentration profiles at and near the left wall as a function of time in Figure 4 show higher particle concentration near the wall, falling as the centre of the riser is approached. Similar observations were reported by Manyele et al. (12) and Li Huilin et al. (21). The present model correctly predicts the trend of particle concentrations. As time progresses, their concentration drops from 0.48 at t = 0 s to 0.054 at t = 0.7 s, while descending from a cluster mid-point coordinate, z, of 0.9 m to z = 0.2 m, respectively. It is evident that considerable dilution of the cluster is predicted to take place. Note that the present model does not take inter-particle forces into account, which may in practice help to keep clusters intact (20). The change in cluster voidage did not greatly affect the evolution of cluster shape.

Figures 5(a) and (b) show average lateral distributions of gas and particle velocities at various times. The particle motion closely follows the upward-flowing carrier gas in the centre, but, near the left wall, particles were observed to descend. Hence, both graphs can be divided into two regions: (a) Region I, distance from left wall < 0.05 m (presence of cluster at wall) and, (b) Region II, distance from left wall > 0.05 m (towards the center of the riser). It was observed that with increasing time, the velocity profiles for both gas and solids approach symmetry at the centre.

Figure 6 shows the lateral variation of cluster width for U_g = 5.5 m/s and varying solids flux. Initially centered at height, z = 0.9 m above the inlet, clusters at the wall were considered with an initial width of 30 mm. As a cluster descends along the wall, its maximum width progressively increases and reaches nearly 120 mm at z = 0.2 m. Beyond this point, the cluster detaches from the wall and is large enough to either fall down or be entrained by the incoming gas. Similar monotonically increasing cluster dimensions were observed for different inlet solid mass fluxes. Mostoufi and Chaouki (22) and Li Huilin et al. (21) found a similar trend from their experimental and numerical investigations, respectively.

Figure 7 shows the cluster velocity of descent as a function of initial cluster width. Simulations were first carried out for widths of 22.2, 26.6, 28.1, 30.0 and 35.6 mm. Both the experimental data (6) and CFD predictions were observed to fluctuate. Interestingly, the predicted data followed a similar trend to the experimental results. When further simulations were conducted for widths of 19.9, 21.0, 23.4 and 31.9 mm, the model captured the experimental trend reasonably well. It is recommended that further investigations be carried out to understand the reasons for the fluctuations.

Figures 8(a) and (b) plot the velocity of descent of a cluster as a function of superficial gas velocity and solid mass flux rate. As the gas velocity and solid flux increase, there is little variation in the predicted descent velocity of the clusters. However, descending clusters experience some drag resistance owing to the rapid upward suspension flow, and hence a small decrease in cluster descending velocity is observed. Similar observations were made by Zhou et al. (5), Lim et al. (6) and Noymer (23).

NOTATION

D_c	width of the cluster [mm]
d_p	particle diameter [μm]
G_s	solid mass flux [kg/m^2.s]
U_{cl}	cluster descent velocity [m/s]
U_g	gas superficial velocity [m/s]
U_p	particle velocity [m/s]
t	time [s]
z	height of the riser [m]
ε	solid volume fraction [-]
ρ	density [kg/m^3]

CONCLUSIONS

A gas-solid Eulerian-Granular CFD model was developed to predict the motion of initially parabolic-drop-shaped clusters at the wall of a CFB riser. The predicted velocity of cluster descent is in reasonable agreement with experimental data of Zhou et al. (6) and Lim et al. (7). Clusters are predicted to distort while descending, from parabolic to drop-shape to petal and back to parabolic, before detaching from the wall. They also increase in size and become more dilute as they accelerate from rest while descending. The present model can be refined in the future by incorporating such additional features as frictional forces, turbulence and interactions between multiple clusters.

REFERENCES

[1] Grace, J.R. and Tuot, J.A., 1979. A theory for cluster formation in vertically conveyed suspension of intermediate density Trans. Int. Chem. Eng., 57, 49–54.

[2] Yerushalmi, R.G.J., Cankurt, N.T., Geldart, D., Liss, B., 1978. Flow regimes in vertical gas– solid contact systems, AIChE Symp. 74, 1–13.

[3] Chen, C.J., 1999. Experiments that address phenomenological issues in fast fluidization, Chem. Eng. Sci. 54, 5529–5539.

[4] Guenther, C. and R. Breault, R., 2007. Wavelet Analysis to Characterize. Cluster Dynamics in a Circulating Fluidized Beds, Powder Technol., 2007; 173, 163–173.

[5] Zhou, J., Grace, J.R., Lim, C.J., Brereton, C.M.H., 1995. Particle velocity profiles in a circulating fluidized red riser of square cross-section, Chem. Eng. Sci., 50 (2), 237-244, 1995.

[6] Lim, K.S., Zhou, J., Finley, C., Grace, J.R., Lim, C. J., & Brereton, C. M. H., 1997. Cluster descending velocity at the wall of circulating fluidized bed risers. Proceedings of the fifth international conference on circulating fluidized beds. Beijing, People's Republic of China.

[7] Horio, M. and Kuroki, H., 1994. Three-dimensional flow visualization of dilutely dispersed solids in bubbling and circulating fluidized beds, Chem. Eng. Sci. 49, 2413–2421.

[8] Soong,C.H., Tuzla,K., Chen, J.C., 1995. Experimental determination of clusters size and velocity in circulating fluidized beds, in: J.F. Large, C. Laguerie (Eds.), Fluidization VIII, AIChE, New York, pp. 219–227.

[9] Sharma, A.K., Tuzla, K., Matsen, J., Chen, J.C., 2000. Parametric effects of particle size and gas velocity on cluster characteristics in fast fluidized beds, Powder Technol. 111, 114–122.

[10] Moortel, V.D., Azario,E., Santini, R., Tadrist, L.1998. Experimental analysis of the gas particle flow in a circulating fluidized bed using a phase Doppler particle analyzer, Chem. Eng. Sci. 53, 1883–1899.

[11] Noymer, P.D., Glicksman, L.R., 1998. Cluster motion and particle-convective heat transfer at the wall of a circulating fluidized bed, Int. J. Heat Mass Transfer 41, 147–158.

[12] Manyele, S.V., Parssinen, J.H., Zhu, J.X., 2002. Characterizing particle aggregates in a high-density and high-flux CFB riser, Chem. Eng. J. 88, 151–161.

[13] Yerushalmi, R.G.J., Turner, D.H., Squires, A.M., 1976. Ind. Eng. Chem. Process Des. Dev., 15, 47–53.

[14] Rhodes, M., Mineo, H., & Hirama, T., 1992. Particle motion at the wall of a circulating fluidized bed. Powder Technology, 70, 207-214.

[15] Shuyan, W., Guodong, L., Yanbo, W., Juhui, C., Yongjian, L., Lixin, W., 2010. Numerical investigation of gas-particle cluster convective heat transfer in circulating fluidized beds, Int. J. Heat and Mass Transfer, 53, 3102 -2110.
[16] Syamlal, M., Rogers, W., O'Brien, T.J., 1993. MFIX Documentation: Theory Guide. National Technical Information Service, vol. 1. Springfield, VA, DOE/METC-9411004, NTIS/DE9400087.
[17] Ansys-Fluent 12.1 Users Guide, Fluent Inc., Lebanon, NH, 2009.
[18] Kuipers, J. A. M., Prins,W., Van Swaaij, W. P. M., 1992. Numerical calculation of wall-to-bed heat transfer coefficients in gas-fluidized beds, AIChE J., 38 (7), 1079 – 1091.
[19] Lun, C.K.K., Savage, S.B., Jeffrey, D.J., Chepurniy, N., 1984. Kinetic theories for granular flow: inelastic particle in Couette flow and slightly inelastic particles in a general flow field. Journal of Fluid Mechanics 140, 223–256.
[20] Shaffer, F., Gopalan, B., Breault, R., Cocco, R., Hays,R., Karri, R., Knowlton, T. A., New View of Riser Flow Fields using High Speed Particle Imaging, NETL Multiphase Flow Workshop May 4-6, 2010.
[21] Huilin, L., Qiaoqun, S., Yurong, H., Yongli, S., Ding, J., Xiang, L., 2005. Numerical study of particle cluster flow in risers with cluster-based approach. Chem. Eng. Sci. 60, 6757-6767.
[22] Mostoufi, N., Chaouki, J., 2004. Flow structure of the solids in gas–solid fluidized beds. Chem. Eng. Sci. 59, 4217 – 4227.
[23] Noymer, P. D., 1997. Heat transfer by particle convection at the wall of a circulating fluidized bed. Ph.D. thesis, Massachusetts Institute of Technology, Cambridge, MA.

Table 1. Kinetic model specifications

Granular temperature, m^2/s^2	10^{-5} [17,18]
Granular viscosity, kg/m. s	Syamlal-O'Brien (16)
Granular bulk viscosity, kg/m. s	Lun et al. (19)
Frictional viscosity, kg/m. s	None
Solids pressure , Pa	Lun etal. (19)
Radial distribution correction factor for inter-particle collisions)	Lun etal. (19)
Elasticity modulus, Pa	Derived (17)
Packing limit, [-]	0.6

Table 2. Parameters used in the CFD simulations

Parameter	**Value(s)**
Height of riser computational domain, m	8, 1.0
Width of riser, m	0.146 and 0.285
Particle diameter, d_p, μm	213
Width of cluster, D_c, mm	19.1, 21, 22.2, 23.4, 26.6, 28.1, 30.2, 31.9 and 35.6
Density of particles, ρ_p, kg/m^3	2640
Inlet solids mass flux, G_s, kg/m^2.s	10, 20, 30, 40 and 60
Superficial gas velocity, U_g, m/s	4.5, 5.5, 6, 7 and 8
Particle-particle coefficient of restitution, [-]	0.95
Volume fraction of particles in cluster, [-]	0.48 (base case)

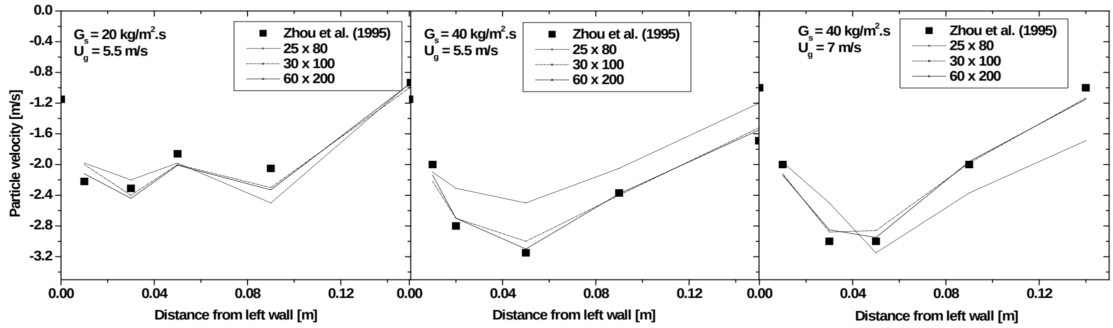

(a) (b) (c)

Figure 1. Grid independent test: Lateral profiles of particle velocities for D_{cl} = 30 mm, d_p = 213 μm, z= 6.2 m, t = 5.2 s]

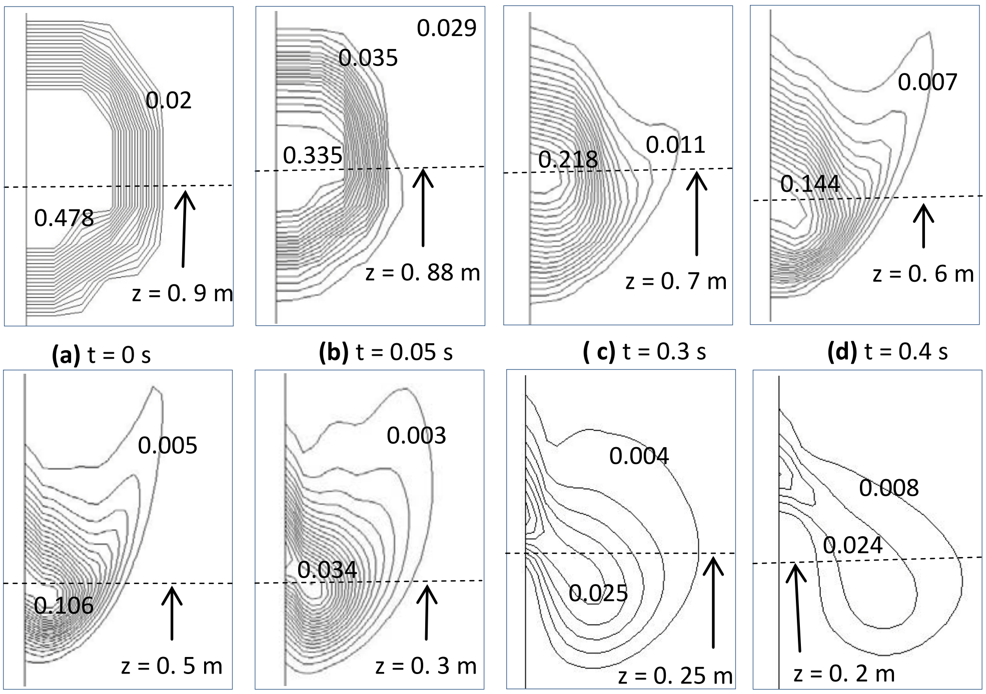

(a) t = 0 s **(b)** t = 0.05 s **(c)** t = 0.3 s **(d)** t = 0.4 s

(e) t = 0.5 s **(f) t** = 0.7 s **(g)** t = 0.75 s **(h)** t = 0.8 s

Figure 2. Volume fraction of particles at instantaneous time, G_s = 10 kg/m^2.s; U_g = 5.5 m/s; D_{cl} = 30 mm

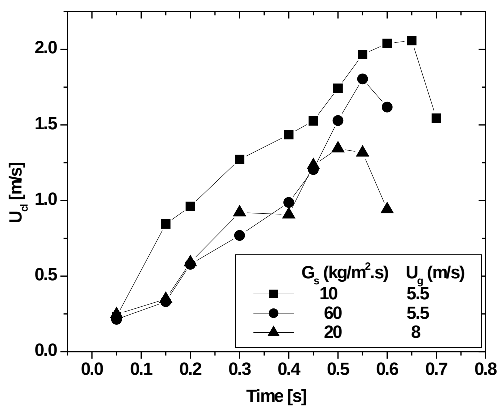

Figure 3. Descent velocity of cluster versus time with varying U_g and G_s

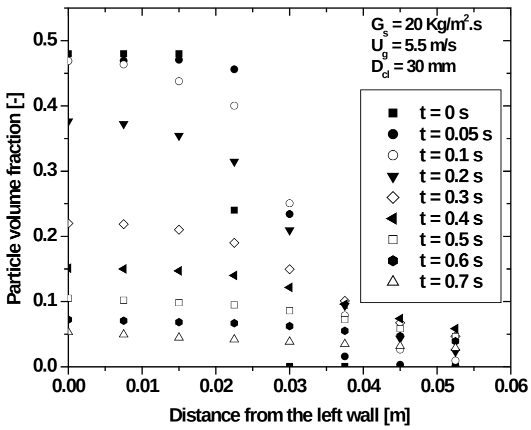

Figure 4. Lateral profile of particle concentration at and near left wall

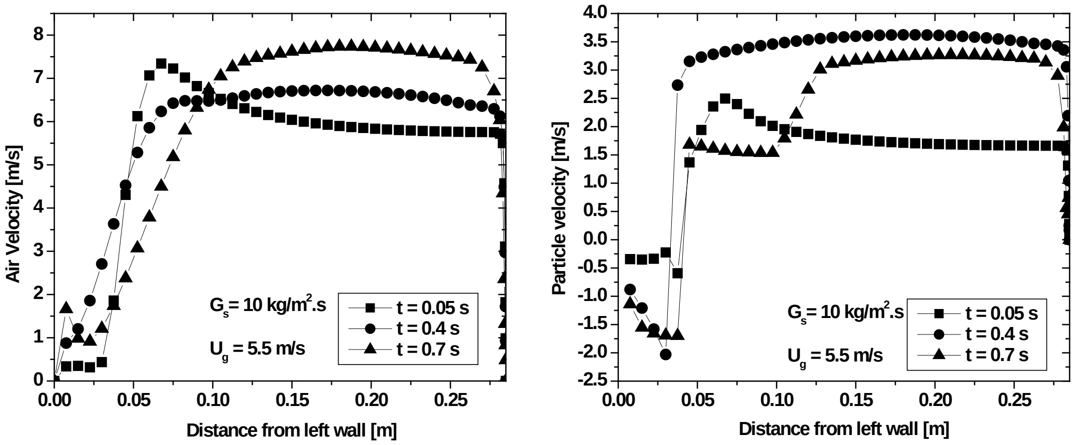

(a) (b)

Figure 5. Lateral distributions of (a) Gas velocity and, (b) Particle velocity at z = 0.5 m, D_{cl} = 30 mm

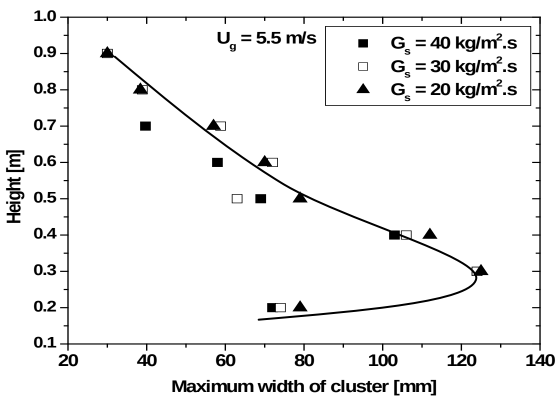

Figure 6. Variation of maximum width of cluster versus height of riser

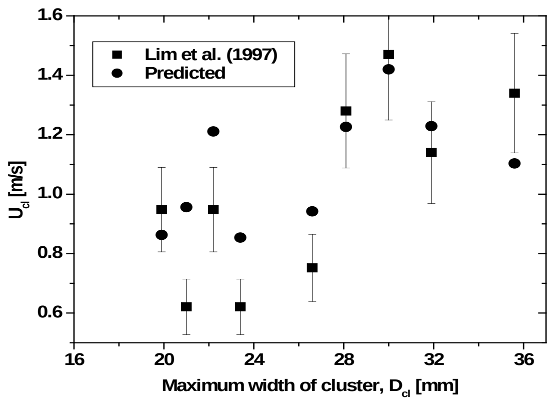

Figure 7. Comparison of predicted cluster descent velocity with experimental data of Lim et al. (1997) including 15% error bars, G_s = 10 kg/m^2.s, U_g = 5.5 m/s.

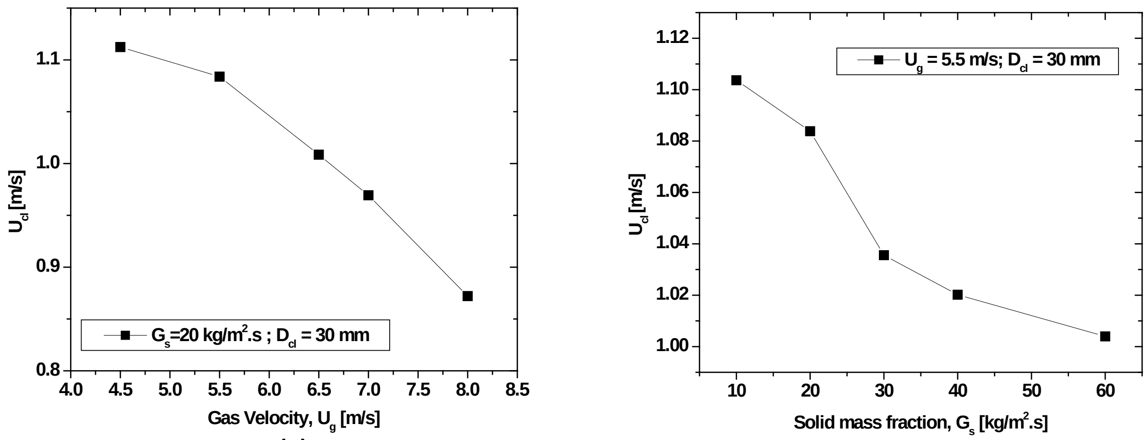

Figure 8. Variation of cluster velocity as a function of (a) Gas velocity and, (b) Solid mass flux at z = 0.5 m